

DriveGPT: Scaling Autoregressive Behavior Models for Driving

Xin Huang[†] Eric M. Wolff[‡] Paul Vernaza Tung Phan-Minh
 Hongge Chen David S. Hayden Mark Edmonds Brian Pierce
 Xinxin Chen Pratik Elias Jacob Xiaobai Chen Chingiz Tairbekov
 Pratik Agarwal Tianshi Gao Yuning Chai Siddhartha Srinivasa[†]
 Cruise LLC

{cyrus.huang, eric.wolff, sidd.srinivasa}@getcruise.com

Abstract

We present *DriveGPT*, a scalable behavior model for autonomous driving. We model driving as a sequential decision making task, and learn a transformer model to predict future agent states as tokens in an autoregressive fashion. We scale up our model parameters and training data by multiple orders of magnitude, enabling us to explore the scaling properties in terms of dataset size, model parameters, and compute. We evaluate *DriveGPT* across different scales in a planning task, through both quantitative metrics and qualitative examples including closed-loop driving in complex real-world scenarios. In a separate prediction task, *DriveGPT* outperforms a state-of-the-art baseline and exhibits improved performance by pretraining on a large-scale dataset, further validating the benefits of data scaling.

1. Introduction

Transformer-based foundation models have become increasingly prevalent in sequential modeling tasks across various machine learning domains. These models are highly effective in handling sequential data by capturing long-range dependencies and temporal relationships. Their success has been evident in natural language processing [16], time-series forecasting [31], and speech recognition [14], where sequential patterns play a crucial role. One of the key strengths of transformer-based models is their capacity to learn from large datasets including millions of training examples, enabling them to address complex tasks with increased model sizes, up to billions of model parameters.

In the context of autonomous driving, transformer-based models have demonstrated great success in behavior modeling [7, 22, 23]. Behavior modeling predicts future actions

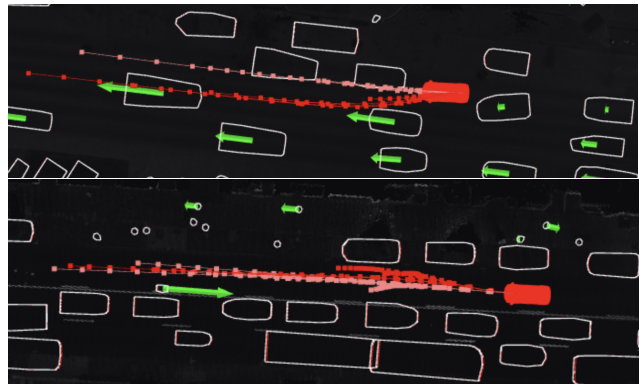


Figure 1. Through data and model scaling, DriveGPT (red) handles complex real-world driving scenarios, such as lane changing in heavy traffic and yielding to a cyclist in the opposite lane, compared to a smaller baseline trained on less data (pink).

of traffic agents to support critical tasks such as planning and motion prediction. Unlike traditional machine learning approaches that may rely on handcrafted features or specific rules, transformers are effective at learning the underlying spatiotemporal dependencies of agent behavior from large-scale multimodal data.

Scaling up model and dataset sizes has been critical for recent advances in sequential modeling for text prediction [12], yet it remains an open question whether these scaling trends hold for the task of behavior modeling. Existing work is often limited by the training data or the model size, as summarized in Table 1.

In our work, we present a comprehensive study of scaling up data sizes and model parameters in the context of autonomous driving. Specifically, we train a transformer-based autoregressive behavior model on over 100 million high-quality human driving examples, ~ 50 times more than existing open-source datasets, and scale the model over 1B parameters, outsize existing published behavior models.

As we scale up the volume of training data and the num-

^{†‡} Corresponding authors.

Model	Parameters	Training Segments
VectorNet [4]	72K	211K
PlanTF [1]	2.1M	1M
QCNet-Argo2 [32]	7.3M	200K
QCNet-WOMD [32]	7.5M	2.2M
Wayformer [18]	20M	2.2M
MotionLM [22]	27M	1.1M
MTR [23]	66M	2.2M
GUMP [8]	523M	2.6M
DriveGPT (Ours)	1.4B	120M

Table 1. DriveGPT is $\sim 3x$ larger and is trained on $\sim 50x$ more data sequences than existing published behavior models.

ber of model parameters, we observe improvements in both quantitative metrics and qualitative behaviors. More importantly, large models trained on extensive, diverse datasets can better handle rare or edge-case scenarios, which often pose significant challenges for autonomous vehicles, as shown in Fig. 1. As a result, we see great potential in scaling up behavior models through data and model parameters to improve the safety and robustness of autonomous driving systems.

Our main contributions are as follows:

1. We present DriveGPT, a large autoregressive behavior model for driving, by scaling up both model parameters and real-world training data samples.
2. We determine empirical driving scaling laws for an autoregressive behavior model in terms of model parameters, data size, and compute. We validate the value of more training data through data scaling that spans two orders of magnitude and compute scaling that spans five orders of magnitude. Our model scaling experiments demonstrate better scalability of autoregressive decoders compared to one-shot decoders.
3. We quantitatively and qualitatively compare models from our scaling experiments to validate their effectiveness in real-world driving scenarios.
4. We demonstrate the generalizability of our model on the Waymo Open Motion Dataset, which outperforms prior state-of-the-art on the motion prediction task and achieves improved performance through large-scale pre-training.

2. Related Work

2.1. Behavior Modeling

Behavior modeling is a critical task in autonomous driving, which covers a broad spectrum of tasks including planning, prediction, and simulation. Taking multimodal inputs including agent history states and map information, behavior models predict the future states of these traffic agents, by

reasoning agent dynamics [2, 24], interactions [10, 25], and driving environments [13, 15].

Among all learning-based models, transformers have gained popularity due to their capability to fuse multimodal inputs as encoders [9, 18, 30, 32] and modeling long-range temporal relationships as decoders [22, 23]. Despite the success of transformers in behavior modeling, existing literature is often restricted by the size of model parameters due to limited training data, which fail to capture the full scaling potential of transformer-based models. In our work, we scale up our transformer models to include billions of parameters, by training on a large-scale dataset including more than 100M driving demonstrations, and validate the scalability of transformer-based models in the context of autonomous driving.

2.2. Large Transformer Models

Large transformers have demonstrated great success in sequential modeling tasks, by scaling up model parameters and data sizes [6, 12, 17, 29]. These scaling laws have pushed the boundary of many sequential modeling tasks including natural language processing [16], time-series forecasting [31], and speech recognition [14].

Recent work has studied the scalability of behavior models in the context of motion prediction [22], planning [26], and simulation [8], yet these studies are either constrained by limited data size (up to a couple of million training examples), or focused on a few orders of magnitude in terms of data and model scaling, limiting the potential to draw statistically significant conclusions over a large scaling spectrum.

In this paper, we aim to study the scaling properties in terms of model parameters, data samples, and compute, across a much larger spectrum compared to prior work. More specifically, we target an autoregressive decoder architecture that has been proven to be both scalable as in the LLM literature and effective in generating accurate trajectories for traffic agents [22].

Beyond autonomous driving, there exists a few relevant literature on building large transformer models for robotic tasks [19, 27], which share a similar transformer architecture as our work. Despite their successes, robotics models often share different input features and dynamic models, and operate in different environments, making them difficult to apply directly to driving tasks.

3. Behavior Model

We use a standard encoder-decoder architecture as our behavior model, as shown in Fig. 2. We use transformer-based models as our encoder and decoder backbones due to their scalability in sequential modeling tasks.

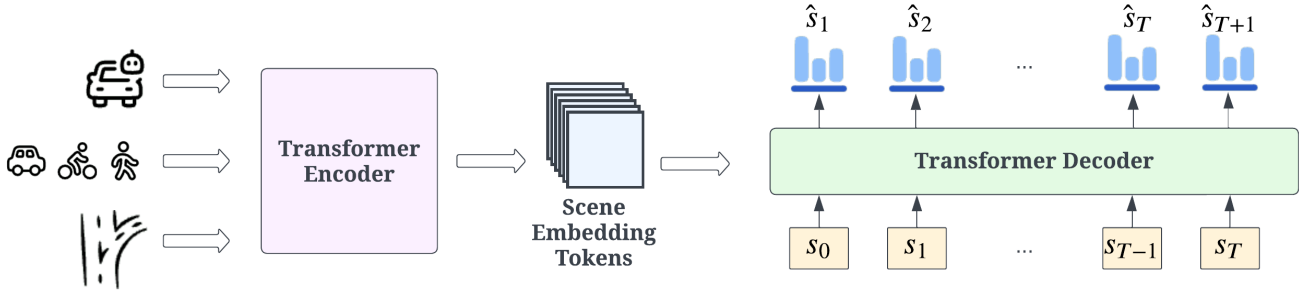


Figure 2. DriveGPT architecture, including a transformer encoder and a transformer decoder. The transformer encoder summarizes relevant scene context, such as target agent history, nearby agent history, and map information, into a set of scene embedding tokens. The transformer decoder follows an LLM-style architecture that takes a sequence of agent states as input and predicts a discrete distribution of actions at the next tick, conditioned on previous states.

3.1. Problem Formulation

We model the problem as a sequential prediction task over the future positions of the target agent up to horizon T , by applying the chain rule at each step, conditioning on driving context information \mathbf{c} and historical agent positions \mathbf{s} :

$$P(s_{1:T}|\mathbf{c}) = \prod_{t=1}^T P(s_t | s_{0:t-1}, \mathbf{c}). \quad (1)$$

The context information includes target agent history states c_{target} , nearby agent history states c_{nearby} , and map states c_{map} . The historical agent information includes agent positions from previous historical steps, i.e. $s_{0:t-1}$ if we want to predict agent positions at step t .

We define “state” as a full kinematic state including position, orientation, velocity, and acceleration, which is commonly available in agent history observations, and “position” as 2-D (x, y) coordinates to simplify the output space.

3.2. Scene Encoder

The encoder follows a standard transformer encoder architecture [23] that fuses all input modalities into a set of scene embedding tokens. It consumes raw input features, including target agent history states, nearby agent history states, and map states as a set of vectors, and normalizes all the inputs to an agent-centric view. Each vector is mapped to a token embedding through a PointNet-like encoder as in [4]. At the end of the encoder, we apply a self-attention transformer [28] to fuse all input context into a set of encoder embeddings, $\mathbf{c} \in \mathbb{R}^{n \times d}$, where n is the number of vectors and d is the token dimensions, that summarize the driving scene.

3.3. LLM-Style Trajectory Decoder

Inspired by the LLM literature [20], we follow [22] to use a transformer decoder architecture to predict the distribution of agent positions at each step in the future.

The decoder first tokenizes agent positions at all steps into embeddings with dimension d through a linear layer, followed by a LayerNorm layer and a ReLU layer. At each step t , the decoder takes agent embeddings up to t , and cross attends them with the encoder embeddings \mathbf{c} to predict the distribution of agent positions at the next step $t + 1$.

The output is a set of discrete actions a represented as the Verlet action [21, 22], as the second derivative of positions. We can apply the following equation to map Verlet actions to positions:

$$s_{t+1} = s_t + (s_t - s_{t-1}) + a_t, \quad (2)$$

where a_t is the predicted Verlet action, and $(s_t - s_{t-1})$ is the estimated velocity. This representation helps predict smooth trajectories using a small set of action candidates.

3.4. Training

To train a DriveGPT model, we follow teacher forcing by applying ground truth future positions as inputs to the trajectory decoder. This allows us to predict all future steps in parallel.

We use a single cross-entropy classification loss over the action space, where the target action is selected as the one that is closest to the ground truth future trajectories. We refer the readers to the Appendix for more details.

3.5. Inference

At inference time, we follow a standard LLM setup and roll out a trajectory over horizon T autoregressively, by repeating the process of predicting the action distribution at the next step, sampling an action, and adding it back to the input sequence.

We sample multiple trajectories in batch to approximate the distribution and then subsample to the desired number of modes using K -Means, as in [22].

4. Scaling Experiments

The goal of our scaling experiments is to determine the effect of model and data size on behavior prediction performance. Quantifying scaling laws similar to those seen in LLMs [12] can help prioritize the value of data and compute for future research directions in behavior modeling. We focus our effort on exploring the next frontier of model and data size — over an order of magnitude beyond previously reported work.

Large-scale driving dataset From millions of miles of high-quality real-world human driving demonstrations, we curated a small subset of 120M segments for an internal research dataset. The dataset is balanced to cover diverse geographic regions from multiple cities and countries, and a variety of driving scenarios, such as passing a double-parked vehicle, unprotected left turns, construction zones, etc. We extracted map information, target agent states, and nearby agent states into vectorized representation, as customary in behavior modeling literature [4].

We scale the model size across three orders of magnitude, from 1.5 million to 1.4 billion parameters, by increasing the embedding dimension. For each model size, we explore multiple learning rate schedules and select the one that yields the best performance. Consistent with practices in large language model scaling [12], each model is trained for a single epoch.

We measure model performance through validation loss computed over a comprehensive validation set. We use validation loss as a proxy to measure model performance, following standard practices in scaling studies [6, 12, 17]. This loss, calculated as cross-entropy on next-action prediction, serves as our primary performance metric. Additional driving-specific metrics are reported in Sec. 5.1.1 and Sec. 5.1.2.

4.1. Data Scaling

Data scaling results are summarized in Fig. 3. The smallest dataset of 2.2M samples mimics the size of Waymo Open Motion Dataset (WOMD) [3], a large open-source dataset for behavior modeling ($\sim 44k$ scenarios with multiple target agents per scenario). Additionally, we select a few subsets of our internal research dataset to study data scaling across different orders of dataset sizes. Our experiments use $\sim 50x$ more data than WOMD, exploring a new region of the design space.

The results indicate that as the model is trained on more unique data samples, the performance improves, regardless of model size. Extrapolating from the scaling law in Fig. 3, to improve the best loss by another 10%, we would need to include 200M more training examples. A 20% improvement would require about 900M more examples. As a re-

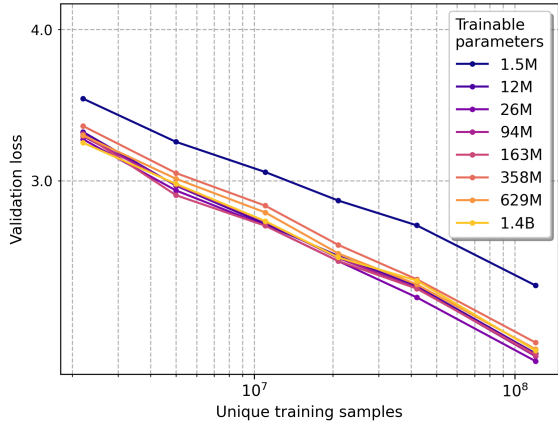


Figure 3. Performance increases with dataset size across a range of model parameters, indicating that data is a limiting factor. Both axes are on a log scale. An exponential fit was applied to all data points except for the 1.5M curve, resulting in the following relationship: $\log(L) = -0.101 \log(D) + 2.656$ with an R^2 value of 0.9902, where L is the validation loss and D is the number of unique training samples.

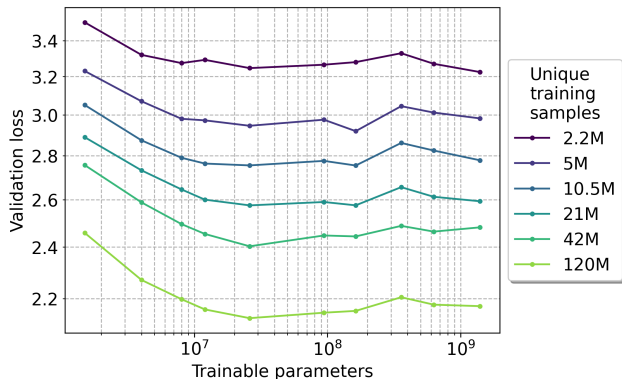


Figure 4. Validation loss saturates with increasing model size across all datasets — in contrast to LLM scaling literature.

sult, we find that data remains to be the bottleneck for further improving driving performance.

Lastly, the scaling results remain relatively consistent across model sizes. This consistency indicates that data scaling comparisons can be done on reasonably small model sizes beyond 10M parameters.

4.2. Model Scaling

We now study model sizes across three orders of magnitude (1.5M to 1.4B parameters). We increase model size by increasing the hidden dimensions of transformers for simplicity. We notice that modifying other parameters such as number of attention heads and hidden dimensions per head do not lead to noticeable changes in the results.

Training larger models is sensitive to learning rates, as

observed in other scaling studies [6, 12]. For each model size, we run multiple experiments at different learning rates to select the one with the optimal performance. We defer more detail in the Appendix.

Results in Fig. 4 show that for a fixed dataset size, increasing model parameters has a mixed effect on the validation loss. The losses improve up to 26M parameters, before hitting a plateau up to 163M parameters. While these results contrast with the LLM scaling literature [12], which shows significant benefits from model scaling, we notice that actual driving metrics continue to improve as model scales, as shown in Sec. 4.4 and Sec. 5.1.2. Further investigation is required to determine the gap between loss and metric measures, and whether there exist fundamental differences in the behavior prediction vs text prediction task.

4.3. Compute Scaling

In Fig. 5, we examine how compute affects training loss, where compute is measured by Floating Point Operations (FLOPs). We identify a monotonically decreasing “min-bound” boundary, which shows the lowest training loss observed up to the current compute value. As we increase compute, training loss generally decreases. Initially, this decrease is quite steep, but it gradually slows down at higher FLOPs values. This trend is consistent with observations in the LLM scaling literature, such as those reported by [6], covering a subset of the full FLOP range explored in these studies.

Next, we investigate if there is an optimal combination of model parameters and data size for a fixed compute budget. Given the large computational expense for training models at the scales we are exploring, it is important to make the best use of our data. In this study, we fixed the compute budget at different FLOP groups. For a fixed compute budget, we can allocate resources either to model parameters or data samples, keeping their product constant.

Fig. 6 plots performance with different compute budgets. The trend clearly shows that a larger compute budget leads to better performance, with optimal model size increasing accordingly, as indicated by the “best” gray line. The results further reveal that data is the main bottleneck, as the smallest model size performs best at the three largest FLOP groups.

4.4. Ablation Study on Decoder Architecture

We scale up two different model architectures by two orders of magnitude: our autoregressive decoder and a one-shot decoder. For the one-shot decoder, we follow [18] to use a transformer decoder that takes a set of learned queries and cross attends them with scene embeddings to produce trajectory samples. This decoder is referred to as “one-shot” because it generates the full trajectory rollout at once, where an autoregressive decoder follows an LLM-style to produce

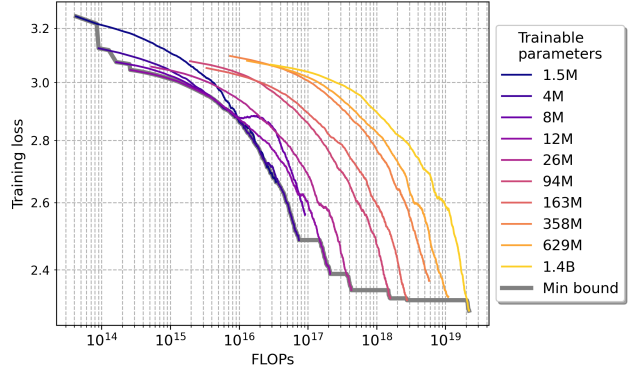


Figure 5. Relationship between (smoothed) training loss and FLOPs. Each curve represents an experiment corresponding to a specific model size, and the “min bound” indicates the best performance possible for a given FLOP budget.

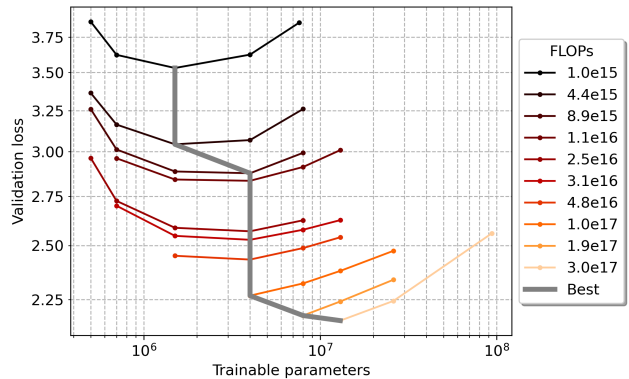


Figure 6. Performance as a function of model size for fixed compute budgets. The solid gray line connects the best result from each compute budget.

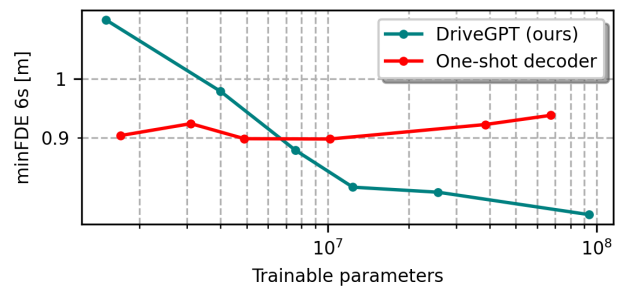


Figure 7. DriveGPT achieves better scalability in terms of minFDE, by adopting an autoregressive architecture compared to a one-shot architecture.

trajectories one step at a time.

The results are summarized in Fig. 7, where we use minFDE at 6 seconds as a proxy to measure the model performance because of different loss definitions between two

Data	$\widehat{\text{mADE}} \downarrow$	$\widehat{\text{mFDE}} \downarrow$	$\widehat{\text{MR}} \downarrow$	$\widehat{\text{Offroad}} \downarrow$	$\widehat{\text{Collision}} \downarrow$
2.2M	1.000	1.000	1.000	1.000	1.000
21M	0.561	0.496	0.420	0.326	0.269
85M	0.496	0.441	0.332	0.238	0.217
120M	0.489	0.433	0.317	0.198	0.196

Table 2. As we scale up more training data, DriveGPT produces better AV trajectories as measured across all metrics. Metrics are normalized to highlight relative performance.

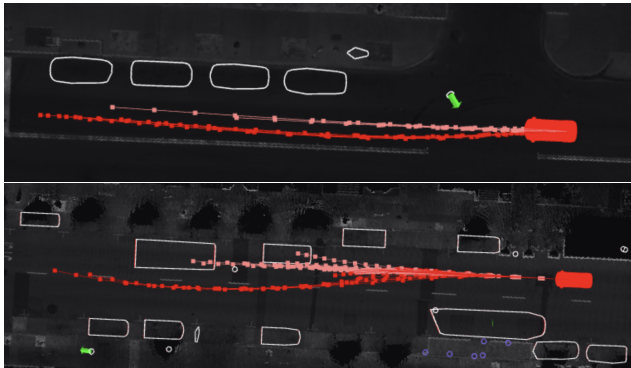


Figure 8. By training on 50x more data, DriveGPT is able to produce high-quality trajectories in red that keep a safe lateral distance from a jaywalker (top) and go around two double-parked vehicles (bottom).

decoder architectures. Despite worse performance at small-scale parameters, our autoregressive decoder achieves better scalability and outperforms the one-shot baseline beyond 8M parameters. While we find it harder to scale the one-shot decoder, we confirm that our autoregressive decoder scales up to 100M parameters in terms of prediction accuracy, and defer further scalability study on the one-shot decoder as future work.

5. Planning and Prediction Experiments

In this section, we show detailed results of DriveGPT in a planning task using our internal research dataset and a motion prediction task using an external dataset. The results here further explore the impact of scaling from Section 4 and help ground those results in driving tasks and metrics.

5.1. Internal Evaluation: AV Planning

For the planning task, we train our model using our internal research dataset, composed of millions of high-quality human driving demonstrations, and generate AV trajectories by autoregressively predicting the next action, as described in Sec. 3.5.

We approximate the distribution by oversampling trajectories in batch and subsampling to 6 trajectories as in [22].

Model	$\widehat{\text{mADE}} \downarrow$	$\widehat{\text{mFDE}} \downarrow$	$\widehat{\text{MR}} \downarrow$	$\widehat{\text{Offroad}} \downarrow$	$\widehat{\text{Collision}} \downarrow$
8M	1.000	1.000	1.000	1.000	1.000
26M	0.954	0.950	0.902	0.858	0.915
94M	0.937	0.925	0.866	0.815	0.890
163M	0.943	0.925	0.875	0.815	0.817

Table 3. As we scale up more model parameters, all metrics improve up to 94M. Collision rate continues to improve at 163M. Metrics are normalized to highlight relative performance.

While the AV must ultimately select a single trajectory for planning, returning multiple samples helps better understand multimodal behavior and aligns with motion prediction metrics.

We measure the planning performance on a comprehensive test set through a set of standard geometric metrics including minADE (mADE), minFDE (mFDE), and miss rate (MR). Additionally, we use semantic-based metrics including offroad rate (Offroad) that measures the ratio of trajectories that leave the road and collision rate (Collision) that measures the ratio of trajectories overlapping with static agents. We normalize these metrics across experiments to highlight relative performance changes as data size and model parameters scale.

5.1.1 Data Scaling Results

We compare a DriveGPT model at 26M parameters (near-optimal from Sec. 4) trained on datasets of different sizes. The baseline dataset (2.2M) is selected to mimic the training size of a typical behavior modeling dataset such as WOMB.

The results are presented in Table 2, where we see that training on more data samples significantly improves the quality of predicted AV trajectories, in terms of critical semantics metrics in driving including offroad rate and collision rate, as well as geometric metrics. These results are consistent with Sec. 5.1.1.

We further present two qualitative examples in Fig. 8 to illustrate the value of training on more data. In these examples, red trajectories represent DriveGPT trained on 120M samples, and pink trajectories are from the same model trained on 2.2M samples. The examples show that our method produces map-compliant and collision-free trajectories when trained on more data, successfully handling complicated interactions involving a jaywalking pedestrian and two double-parked vehicles.

5.1.2 Model Scaling Results

We train four models using our 120M internal research dataset, and select the 8M model as the baseline. The baseline represents a reasonable size at which our model starts

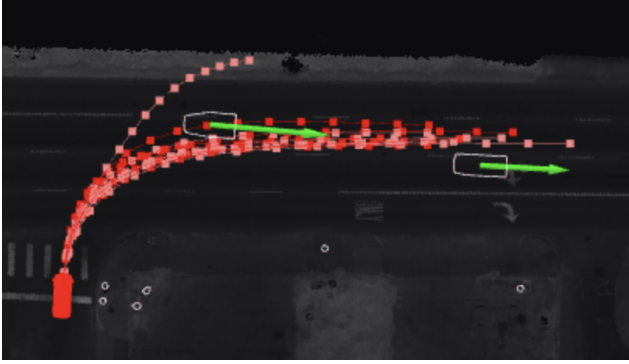


Figure 9. By training with 12x more parameters, DriveGPT (red) produces realistic trajectories that obey lane boundaries when performing a right turn into traffic.

to outperform one-shot decoders, as shown in Sec. 4.4.

The results are presented in Table 3, where all metrics improve as the model size increases up to 94M parameters, with further gains in the collision metric at 163M parameters. Although validation loss stabilizes between 26M and 163M in Fig. 4, driving metrics continue to improve with increased model capacities, highlighting the potential benefits of introducing more parameters for enhanced driving performance.

We present a qualitative example in Fig. 9, where a larger DriveGPT including 94M parameters produces better trajectory samples in red that stay within the road boundary, compared to a smaller version including 8M parameters, in a right turn scenario.

5.1.3 Closed-Loop Driving

We demonstrate the effectiveness of DriveGPT as a real-time motion planner in a closed loop setting. The model takes input features from an industry-level perception system that outputs agent states and map information.

In Fig. 10, we present a challenging example in dense urban traffic where there are two double-parked vehicles blocking the path forward along with other oncoming vehicles. DriveGPT generates smooth and safe trajectories, bypassing the blocking vehicles and moving back to the original lane afterward. More examples are presented in the supplementary material.

5.2. External Evaluation: Motion Prediction

To directly compare with published results, we evaluate DriveGPT on the WOMD motion prediction task. Additionally, we explore the benefits of scale by pretraining on our internal research dataset and finetuning on the significantly smaller WOMD dataset.

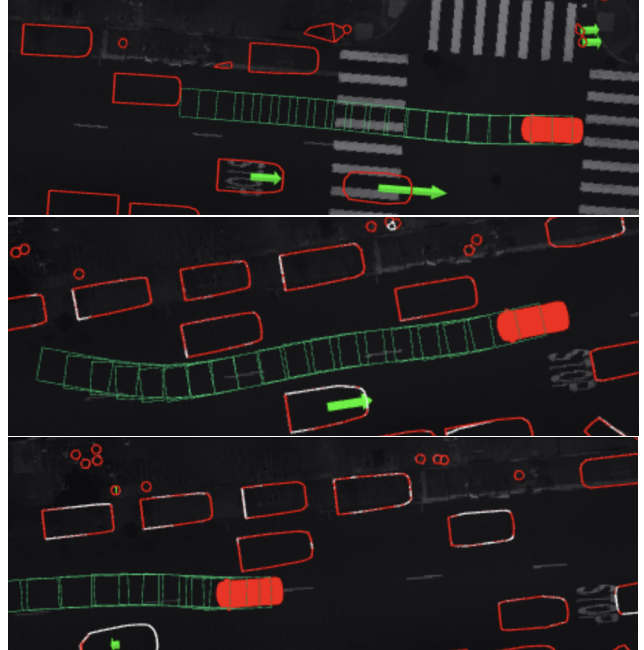


Figure 10. Example of DriveGPT running as a closed-loop planner at real time in dense urban traffic. It first produces a forward trajectory (top), updates it to bypass double-parked vehicles (middle), and drives back to the original lane at the end (bottom).

5.2.1 Open-Source Encoder

For our external evaluation, we use the open-source MTR [23] encoder. This encoder is similar to the one described in Sec. 3.2. We make this change to improve the reproducibility of our results and take advantage of MTR’s open-source dataloading code for WOMD. We use the same autoregressive decoder following [22], as described in Sec. 3.3.

5.2.2 Pretraining Setup

We made a couple of minor modifications to DriveGPT to be compatible with the WOMD dataset. First, we modify our map data to include the same semantics as in WOMD. Second, we modify our agent data to include the same kinematic features for traffic agents as in WOMD.

We pretrain DriveGPT by training on our internal research dataset for one epoch (as in Sec. 4). We load the pre-trained checkpoint and finetune the model using the same training setup as in the MTR codebase [23], where we train the model for 30 epochs using a weighted decay learning rate scheduler.

5.2.3 Validation Results

We measure model performance via a set of standard WOMD metrics, including minADE (mADE), minFDE

Model	Vehicle (2s)				Vehicle (5s)				Vehicle (8s)			
	mADE↓	mFDE↓	MR↓	mAP↑	mADE↓	mFDE↓	MR↓	mAP↑	mADE↓	mFDE↓	MR↓	mAP↑
MTR [23]	0.3292	0.6009	0.1087	0.5400	0.6655	1.3155	0.1463	0.4548	1.2454	2.6178	0.1935	0.3795
DriveGPT-WOMD	0.2875	0.5131	0.0842	0.3951	0.5716	1.0972	0.1180	0.3074	1.0553	2.2434	0.1676	0.2546
DriveGPT-Finetune	0.2866	0.5101	0.0817	0.3825	0.5659	1.0795	0.1136	0.2984	1.0404	2.2069	0.1631	0.2497

Table 4. Compared to a state-of-the-art baseline method, our model achieves better geometric metrics for vehicle prediction using an autoregressive decoder architecture, and even better metrics after pretraining on our internal research dataset.

Pedestrian	mADE↓	mFDE↓	MR↓	mAP↑
MTR [23]	0.3440	0.7193	0.0733	0.4228
DriveGPT-WOMD	0.3086	0.6346	0.0732	0.2908
DriveGPT-Finetune	0.3048	0.6253	0.0696	0.2810
Cyclist	mADE↓	mFDE↓	MR↓	mAP↑
MTR [23]	0.7045	1.4248	0.1836	0.3653
DriveGPT-WOMD	0.6351	1.2849	0.1752	0.2667
DriveGPT-Finetune	0.6253	1.2593	0.1717	0.2339

Table 5. DriveGPT achieves better geometric results in pedestrian and cyclist prediction. Results are averaged over 3 prediction horizons.

(mFDE), miss rate (MR), and mAP. Each metric is measured on the validation set and computed over three different time horizons.

We select MTR [23], a state-of-the-art motion prediction model, as our baseline and reproduce its results using its open-source code. We present two variants of our method to validate its effectiveness on the motion prediction task, including **DriveGPT-WOMD** that is trained on WOMD, and **DriveGPT-Finetune** that is pretrained on our 120M internal research dataset and finetuned on WOMD.

The vehicle prediction results are summarized in Table 4, where we see that our model outperforms MTR in all geometric metrics by a large margin, especially at short horizons (2s and 5s) where we see more than 12% improvements in minADE and minFDE, as well as 20% in miss rate. While we focus more on geometric metrics that emphasize the recall of predicted trajectory samples (i.e. not missing the critical trajectory), our model shows lower mAP scores due to suboptimal probability estimates. These estimates are computed by accumulating log probabilities over a long sequence, which reveals a limitation of using an autoregressive decoder to produce accurate probability estimates, as also noted in the LLM literature [5, 11], and we defer improving the probability estimates as future work.

We observe up to 4% additional gains by pretraining on our internal dataset, despite a large distribution shift between our internal dataset and the public WOMD dataset, in terms of trajectory distributions, feature noises, and dif-

Vehicle	Data	mADE↓	mFDE↓	MR↓
DriveGPT-WOMD	N/A	0.6381	1.2846	0.1233
DriveGPT-Finetune	40M	0.6368	1.2788	0.1217
DriveGPT-Finetune	80M	0.6341	1.2736	0.1207
DriveGPT-Finetune	120M	0.6310	1.2655	0.1195

Table 6. Using more training samples during pretraining gives better results (averaged over 3 horizons) in the finetuned model. This verifies the benefit of data scaling as shown in Sec. 4.1.

ferences in semantic definitions.

Beyond vehicle prediction, we report results in predicting pedestrians and cyclists in Table 5, where we see a similar level of improvements. This validates the generalizability of our method of predicting a diverse set of agent types. Again, we see extra gains by pretraining on our internal research dataset, especially for cyclists.

5.2.4 Data Scaling in Pretraining

We validate the effectiveness of data scaling, by pretraining DriveGPT on various sizes of our internal dataset. The results in Table 6 indicate that pretraining on more unique samples leads to better results in the finetuned model, aligning with our findings in Sec. 4.1 that data scaling improves model performance.

5.2.5 Test Results

We report results on the WOMD test set in Table 7. The results demonstrate that our method outperforms existing state-of-the-art non-ensemble models in terms of geometric metrics. Compared to Wayformer [18] and MotionLM [22] that use ensembles of up to 8 replicas, our model achieves the best minADE and minFDE metrics and the second-best miss rate metric without any ensembling. We observe lower Soft mAP¹ scores from our method due to suboptimal probability estimates, as discussed in Sec. 5.2.3.

Consistent with the results reported in Table 4 and Table 5, we observe additional gains by pretraining on our

¹We report Soft mAP in Table 7 to be consistent with the results reported in [22].

WOMD Test	mADE↓	mFDE↓	MR↓	Soft mAP↑
HDGT [9]	0.7676	1.1077	0.1325	0.3709
MTR [23]	0.6050	1.2207	0.1351	0.4216
HPTR [30]	0.5565	1.1393	0.1434	0.3904
Wayformer Ensemble [18]	0.5454	1.1280	0.1228	<u>0.4335</u>
MotionLM Ensemble [22]	0.5509	1.1199	0.1058	0.4507
DriveGPT-WOMD	<u>0.5290</u>	<u>1.0652</u>	0.1239	0.3244
DriveGPT-Finetune	0.5247	1.0523	<u>0.1204</u>	0.3141

Table 7. On the WOMD test set, DriveGPT achieves better results in geometric metrics without any ensembling, and improved performance after pretraining. Results are averaged over three agent types (vehicle, pedestrian, cyclist) and three prediction horizons (2s, 5s, 8s). The best metric is highlighted in bold and the second best is underlined.

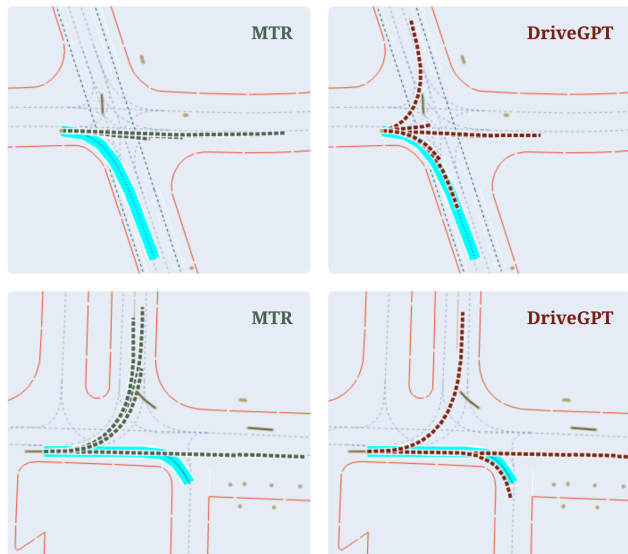


Figure 11. Compared to MTR (left), DriveGPT (right) produces more accurate and diverse trajectories in complex intersections. Blue represents ground truth future trajectories.

internal dataset.

5.2.6 Qualitative Comparison

We present two qualitative comparisons in Fig. 11, where DriveGPT produces better trajectories in terms of diversity (covering more distinct outcomes) and accuracy (matching with the ground truth future) compared to MTR. This improvement is evident in challenging scenarios with limited agent history information (top row) and multiple future modalities (bottom row).

6. Conclusion

We introduced DriveGPT, an LLM-style autoregressive behavior model, to better understand the effects of model and dataset size for autonomous driving. We

systematically explored model performance as a function of both dataset size and model parameters, uncovering LLM-like scaling laws for data and compute scaling, along with limited model scaling properties. We showed the quantitative and qualitative benefits of scaling for planning in real-world driving scenarios. Additionally, we demonstrated our method on a public motion prediction benchmark, where DriveGPT outperformed a state-of-the-art baseline by a large margin and achieved improved performance through pretraining on a large scale dataset.

References

- [1] Jie Cheng, Yingbing Chen, Xiaodong Mei, Bowen Yang, Bo Li, and Ming Liu. Rethinking imitation-based planners for autonomous driving. In *2024 IEEE International Conference on Robotics and Automation (ICRA)*, pages 14123–14130. IEEE, 2024. 2
- [2] Henggang Cui, Thi Nguyen, Fang-Chieh Chou, Tsung-Han Lin, Jeff Schneider, David Bradley, and Nemanja Djuric. Deep kinematic models for kinematically feasible vehicle trajectory predictions. In *2020 IEEE International Conference on Robotics and Automation (ICRA)*, pages 10563–10569. IEEE, 2020. 2
- [3] Scott Ettinger, Shuyang Cheng, Benjamin Caine, Chenxi Liu, Hang Zhao, Sabeek Pradhan, Yuning Chai, Ben Sapp, Charles R Qi, Yin Zhou, et al. Large scale interactive motion forecasting for autonomous driving: The waymo open motion dataset. In *Proceedings of the IEEE/CVF International Conference on Computer Vision*, pages 9710–9719, 2021. 4
- [4] Jiyang Gao, Chen Sun, Hang Zhao, Yi Shen, Dragomir Anguelov, Congcong Li, and Cordelia Schmid. VectorNet: Encoding hd maps and agent dynamics from vectorized representation. In *Proceedings of the IEEE/CVF conference on computer vision and pattern recognition*, pages 11525–11533, 2020. 2, 3, 4
- [5] Jiahui Geng, Fengyu Cai, Yuxia Wang, Heinz Koepl, Preslav Nakov, and Iryna Gurevych. A survey of confidence estimation and calibration in large language models. In *Proceedings of the 2024 Conference of the North American*

- Chapter of the Association for Computational Linguistics: *Human Language Technologies*, pages 6577–6595, 2024. 8
- [6] Jordan Hoffmann, Sebastian Borgeaud, Arthur Mensch, Elena Buchatskaya, Trevor Cai, Eliza Rutherford, Diego de Las Casas, Lisa Anne Hendricks, Johannes Welbl, Aidan Clark, et al. Training compute-optimal large language models. *arXiv preprint arXiv:2203.15556*, 2022. 2, 4, 5, 12
- [7] Yihan Hu, Jiazhi Yang, Li Chen, Keyu Li, Chonghao Sima, Xizhou Zhu, Siqi Chai, Senyao Du, Tianwei Lin, Wenhai Wang, et al. Planning-oriented autonomous driving. In *Proceedings of the IEEE/CVF Conference on Computer Vision and Pattern Recognition*, pages 17853–17862, 2023. 1
- [8] Yihan Hu, Siqi Chai, Zhenning Yang, Jingyu Qian, Kun Li, Wenxin Shao, Haichao Zhang, Wei Xu, and Qiang Liu. Solving motion planning tasks with a scalable generative model. In *European Conference on Computer Vision*, pages 386–404. Springer, 2024. 2
- [9] Xiaosong Jia, Penghao Wu, Li Chen, Yu Liu, Hongyang Li, and Junchi Yan. HDGT: Heterogeneous driving graph transformer for multi-agent trajectory prediction via scene encoding. *IEEE transactions on pattern analysis and machine intelligence*, 2023. 2, 9
- [10] Chiyu Jiang, Andre Cornman, Cheolho Park, Benjamin Sapp, Yin Zhou, Dragomir Anguelov, et al. MotionDiffuser: Controllable multi-agent motion prediction using diffusion. In *Proceedings of the IEEE/CVF Conference on Computer Vision and Pattern Recognition*, pages 9644–9653, 2023. 2
- [11] Zhengbao Jiang, Jun Araki, Haibo Ding, and Graham Neubig. How can we know when language models know? on the calibration of language models for question answering. *Transactions of the Association for Computational Linguistics*, 9:962–977, 2021. 8
- [12] Jared Kaplan, Sam McCandlish, Tom Henighan, Tom B Brown, Benjamin Chess, Rewon Child, Scott Gray, Alec Radford, Jeffrey Wu, and Dario Amodei. Scaling laws for neural language models. *arXiv preprint arXiv:2001.08361*, 2020. 1, 2, 4, 5, 12
- [13] ByeoungDo Kim, Seong Hyeon Park, Seokhwan Lee, Elbek Khoshimjonov, Dongsuk Kum, Junsoo Kim, Jeong Soo Kim, and Jun Won Choi. LaPred: Lane-aware prediction of multimodal future trajectories of dynamic agents. In *Proceedings of the IEEE/CVF Conference on Computer Vision and Pattern Recognition*, pages 14636–14645, 2021. 2
- [14] Sehoon Kim, Amir Gholami, Albert Shaw, Nicholas Lee, Karttikeya Mangalam, Jitendra Malik, Michael W Mahoney, and Kurt Keutzer. Squeezeformer: An efficient transformer for automatic speech recognition. *Advances in Neural Information Processing Systems*, 35:9361–9373, 2022. 1, 2
- [15] Ming Liang, Bin Yang, Rui Hu, Yun Chen, Renjie Liao, Song Feng, and Raquel Urtasun. Learning lane graph representations for motion forecasting. In *Computer Vision—ECCV 2020: 16th European Conference, Glasgow, UK, August 23–28, 2020, Proceedings, Part II 16*, pages 541–556. Springer, 2020. 2
- [16] Ben Mann, N Ryder, M Subbiah, J Kaplan, P Dhariwal, A Neelakantan, P Shyam, G Sastry, A Askell, S Agarwal, et al. Language models are few-shot learners. *arXiv preprint arXiv:2005.14165*, 1, 2020. 1, 2
- [17] Niklas Muennighoff, Alexander Rush, Boaz Barak, Teven Le Scao, Nouamane Tazi, Aleksandra Piktus, Sampo Pyysalo, Thomas Wolf, and Colin A Raffel. Scaling data-constrained language models. *Advances in Neural Information Processing Systems*, 36:50358–50376, 2023. 2, 4
- [18] Nigamaa Nayakanti, Rami Al-Rfou, Aurick Zhou, Kratharth Goel, Khaled S Refaat, and Benjamin Sapp. Wayformer: Motion forecasting via simple & efficient attention networks. In *2023 IEEE International Conference on Robotics and Automation (ICRA)*, pages 2980–2987. IEEE, 2023. 2, 5, 8, 9, 12
- [19] Abby O’Neill, Abdul Rehman, Abhiram Maddukuri, Abhishek Gupta, Abhishek Padalkar, Abraham Lee, Acorn Pooley, Agrim Gupta, Ajay Mandlekar, Ajinkya Jain, et al. Open x-embodiment: Robotic learning datasets and rt-x models: Open x-embodiment collaboration 0. In *2024 IEEE International Conference on Robotics and Automation (ICRA)*, pages 6892–6903. IEEE, 2024. 2
- [20] Alec Radford, Jeffrey Wu, Rewon Child, David Luan, Dario Amodei, Ilya Sutskever, et al. Language models are unsupervised multitask learners. *OpenAI blog*, 1(8):9, 2019. 3
- [21] Nicholas Rhinehart, Kris M Kitani, and Paul Vernaza. R2p2: A reparameterized pushforward policy for diverse, precise generative path forecasting. In *ECCV*, pages 772–788, 2018. 3
- [22] Ari Seff, Brian Cera, Dian Chen, Mason Ng, Aurick Zhou, Nigamaa Nayakanti, Khaled S Refaat, Rami Al-Rfou, and Benjamin Sapp. MotionLM: Multi-agent motion forecasting as language modeling. In *Proceedings of the IEEE/CVF International Conference on Computer Vision*, pages 8579–8590, 2023. 1, 2, 3, 6, 7, 8, 9, 12
- [23] Shaoshuai Shi, Li Jiang, Dengxin Dai, and Bernt Schiele. Motion transformer with global intention localization and local movement refinement. *Advances in Neural Information Processing Systems*, 35:6531–6543, 2022. 1, 2, 3, 7, 8, 9, 12
- [24] Haoran Song, Di Luan, Wenchao Ding, Michael Y Wang, and Qifeng Chen. Learning to predict vehicle trajectories with model-based planning. In *Conference on Robot Learning*, pages 1035–1045. PMLR, 2022. 2
- [25] Qiao Sun, Xin Huang, Junru Gu, Brian C Williams, and Hang Zhao. M2I: From factored marginal trajectory prediction to interactive prediction. In *Proceedings of the IEEE/CVF Conference on Computer Vision and Pattern Recognition*, pages 6543–6552, 2022. 2
- [26] Qiao Sun, Shiduo Zhang, Danjiao Ma, Jingzhe Shi, Derun Li, Simian Luo, Yu Wang, Ningyi Xu, Guangzhi Cao, and Hang Zhao. Large trajectory models are scalable motion predictors and planners. *arXiv preprint arXiv:2310.19620*, 2023. 2
- [27] Octo Model Team, Dibya Ghosh, Homer Walke, Karl Pertsch, Kevin Black, Oier Mees, Sudeep Dasari, Joey Hejna, Tobias Kreiman, Charles Xu, et al. Octo: An open-source generalist robot policy. *arXiv preprint arXiv:2405.12213*, 2024. 2
- [28] Ashish Vaswani, Noam Shazeer, Niki Parmar, Jakob Uszkoreit, Llion Jones, Aidan N Gomez, Łukasz Kaiser, and Illia Polosukhin. Attention is all you need. *Advances in neural information processing systems*, 30(2017), 2017. 3

- [29] Xiaohua Zhai, Alexander Kolesnikov, Neil Houlsby, and Lucas Beyer. Scaling vision transformers. In *Proceedings of the IEEE/CVF conference on computer vision and pattern recognition*, pages 12104–12113, 2022. [2](#)
- [30] Zhejun Zhang, Alexander Liniger, Christos Sakaridis, Fisher Yu, and Luc Van Gool. Real-time motion prediction via heterogeneous polyline transformer with relative pose encoding. In *Advances in Neural Information Processing Systems (NeurIPS)*, 2023. [2](#), [9](#)
- [31] Haoyi Zhou, Shanghang Zhang, Jieqi Peng, Shuai Zhang, Jianxin Li, Hui Xiong, and Wancai Zhang. Informer: Beyond efficient transformer for long sequence time-series forecasting. In *Proceedings of the AAAI conference on artificial intelligence*, pages 11106–11115, 2021. [1](#), [2](#)
- [32] Zikang Zhou, Jianping Wang, Yung-Hui Li, and Yu-Kai Huang. Query-centric trajectory prediction. In *Proceedings of the IEEE/CVF Conference on Computer Vision and Pattern Recognition*, pages 17863–17873, 2023. [2](#)

A. Training Detail

A.1. Internal Evaluation: AV Planning

We train our models on the internal research dataset for 1 epoch, as customary in the LLM scaling literature [6, 12].

Our models follow the implementations described in [18, 22], and are trained using a batch size of 2048 and a standard Adam optimizer adopted in [12]. We follow the optimal learning rate schedule discovered in [6], which applies a cosine decay with a cycle length equivalent to the total number of training steps.

A.2. External Evaluation: Motion Prediction

We train our models on the WOMD data following the same setup in [23]. More specifically, we use a batch size of 80 and an AdamW optimizer with a learning rate of 0.0001. The models are trained for 30 epochs, where the learning rate is decayed by a factor of 0.5 every 2 epochs, starting from epoch 20.

B. Scaling Detail

B.1. Scaling Configurations

In our scaling experiments, we vary the model size through the hidden dimension d_{model} in both encoder and decoder transformers, as summarized in Table. 8. For each model size, we run multiple experiments at different maximum learning rates, and present the optimal value in Table. 8.

B.2. Ablation Study on Attention Heads

In Fig. 12, we present an ablation study examining the impact of the number of heads in the encoder and decoder transformers, while keeping the hidden dimension the same, as specified in Table. 8. For each hidden dimension (d_{model}), we conduct experiments across multiple configurations² of attention heads and present their validation losses using a distinct color. While we notice a pattern where more decoder attention heads lead to better performance for small models, the scaling trend is more influenced by the hidden dimension size than by the number of attention heads when the hidden dimension remains fixed.

B.3. Ablation Study on Decoder Scaling

In Fig. 13, we present model scaling results (in dashed lines) where we only scale up the autoregressive decoder, while keeping the encoder at a fixed size. Compared to scaling both encoder and decoder (in solid lines), scaling only the decoder exhibits a similar trend but yields worse performance, especially for models exceeding 10M parameters. Therefore, our main results focus on scaling both encoder and decoder.

²For the last group, we omit a few models due to memory constraints.

Model Size	Hidden Dimension (d_{model})	Max LR
1.5M	64	0.001
4M	128	0.001
8M	192	0.001
12M	256	0.001
26M	384	0.001
94M	768	0.0003
163M	1024	0.0003
358M	1536	0.0001
629M	2048	0.0001
1.4B	3072	0.0001

Table 8. We vary the model size over three orders of magnitude through hidden dimensions. For each model size, we report the optimal learning rate, which decreases as the model size increases, matching the observations in the LLM scaling literature [6, 12].

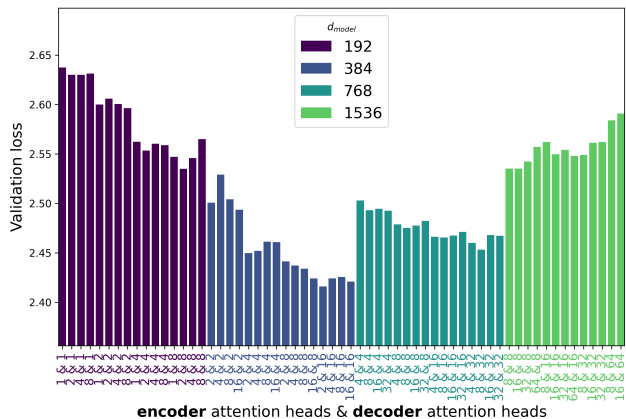


Figure 12. Adjusting the number of attention heads has a smaller effect on the trend of validation losses, compared to changing the hidden dimension.

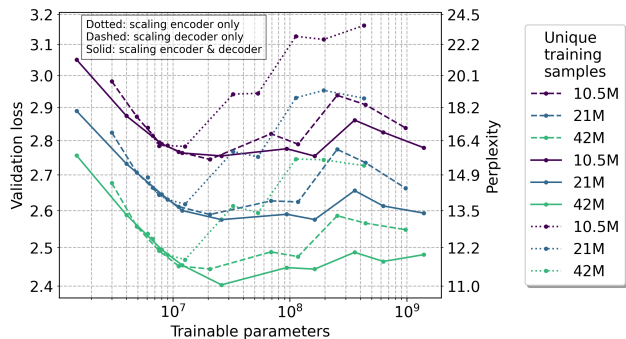


Figure 13. Scaling only the encoder or decoder exhibits a similar trend but worse results compared to scaling both encoder and decoder. Furthermore, encoder only scaling leads to worse results compared to decoder only scaling.

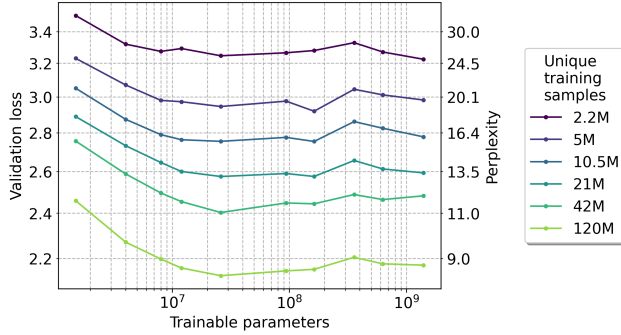


Figure 14. Fig. 4 replotted with a perplexity scale on the right y -axis for ease of reference.

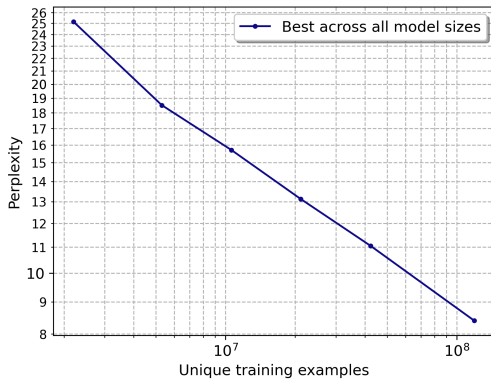


Figure 15. We fit the best perplexity values from all models in Fig. 3 as a function of dataset size. A simple linear regression yields $\log(P) = -0.27 \log(D) + 7.111$ with an R^2 value of 0.9962, where P is the validation perplexity and D is the number of unique training examples.

B.4. Ablation Study on Encoder Scaling

In Fig. 13, we present model scaling results (in dotted lines) where we only scale up the encoder, while keeping the decoder at a fixed size. Similarly, scaling encoder leads to worse performance compared to scaling both encoder and decoder. Furthermore, the performance of scaling the encoder is worse than scaling the decoder.

B.5. Scaling From a Perplexity View

Following the LLM scaling literature, we present our scaling results as a function of validation loss. Another key aspect to highlight is the perplexity scale. Perplexity, defined as the exponentiation of entropy, quantifies how well a probability model predicts a sample. It reflects the effective number of choices the model considers: a perplexity of k implies the model is k -way perplexed.

In Fig. 14, we re-plot the scaling results, adding a secondary y -axis to represent perplexity. We observe that the perplexity decreases by approximately 4 each time the

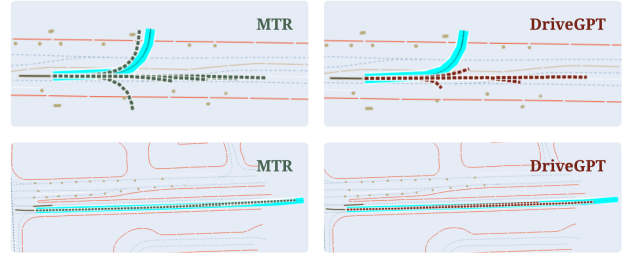


Figure 16. In examples where DriveGPT has the largest error regressions compared to MTR, it predicts less accurate trajectories due to the presence of lane boundary (top row) or missing map information (bottom row). Blue represents ground truth future.

Model Parameters	mADE↓	mFDE↓	MR↓
2M	0.6953	1.4297	0.1489
4M	0.6534	1.3202	0.1298
9M	0.6423	1.2955	0.1249
14M	0.6381	1.2846	0.1233
21M	0.6396	1.2871	0.1225

Table 9. Scaling model parameters in DriveGPT-WOMD improves vehicle prediction metrics up to 14M model parameters. Results are averaged over 3 prediction horizons.

dataset size is doubled, up to the 10.5M dataset. Beyond this point, doubling the dataset size yields diminishing returns.

In Fig. 15, we plot the perplexity of our best models as a function of unique training examples. Extrapolating from the perplexity fit in the figure, a perplexity of 7 would require 80M more training examples and a perplexity of 5 would require 600M more training examples.

C. Additional Qualitative Examples

C.1. Additional Closed-Loop Driving Examples

In the supplementary video³, we present additional examples of using DriveGPT as a real-time motion planner in a closed loop setting. The video covers representative challenging scenarios in driving, including a) unprotected left turn, b) double parked vehicle, c) construction zone, d) blow-through cyclist, and e) lane change in heavy traffic.

C.2. Failure Cases on WOMD

We show two representative failure examples of DriveGPT in Fig. 16, selected based on the largest minFDE regressions of our method compared to the MTR baseline on WOMD. In the first example (top row), our method fails to predict trajectories that make a left turn, likely due to the presence of a lane boundary. In the second example (bottom

³<https://youtu.be/-hLi44PFY8g>

row), DriveGPT predicts an undershooting trajectory that results in a larger longitudinal error due to missing map information in the data.

D. WOMD Model Scaling

We present an ablation study on model scaling using DriveGPT-WOMD in Table 9. The results show that the model performance continues to improve up to 14M parameters, with no further gains beyond this point due to the limited sample size in WOMD. Therefore, we choose to report the results from the 14M model in Sec. 5.2.